

## Influence of fly ash cenospheres on performance of coir fiber-reinforced recycled high-density polyethylene biocomposites

Sukanya Satapathy, Raju V. S. Kothapalli

Polymers and Functional Materials Division, CSIR-Indian Institute of Chemical Technology, Hyderabad-500007, Telangana, India  
Correspondence to: S. Satapathy (E-mail: sukanya@iict.res.in)

**ABSTRACT:** Recycled high-density polyethylene (RHDPE)/coir fiber (CF)-reinforced biocomposites were fabricated using melt blending technique in a twin-screw extruder and the test specimens were prepared in an automatic injection molding machine. Variation in mechanical properties, crystallization behavior, water absorption, and thermal stability with the addition of fly ash cenospheres (FACS) in RHDPE/CF composites were investigated. It was observed that the tensile modulus, flexural strength, flexural modulus, and hardness properties of RHDPE increase with an increase in fiber loading from 10 to 30 wt %. Composites prepared using 30 wt % CF and 1 wt % MA-g-HDPE exhibited optimum mechanical performance with an increase in tensile modulus to 217%, flexural strength to 30%, flexural modulus to 97%, and hardness to 27% when compared with the RHDPE matrix. Addition of FACS results in a significant increase in the flexural modulus and hardness of the RHDPE/CF composites. Dynamic mechanical analysis tests of the RHDPE/CF/FACS biocomposites in presence of MA-g-HDPE revealed an increase in storage ( $E'$ ) and loss ( $E''$ ) modulus with reduction in damping factor ( $\tan \delta$ ), confirming a strong influence between the fiber/FACS and MA-g-HDPE in the RHDPE matrix. Differential scanning calorimetry, thermogravimetric analysis thermograms also showed improved thermal properties in the composites when compared with RHDPE matrix. The main motivation of this study was to prepare a value added and low-cost composite material with optimum properties from consumer and industrial wastes as matrix and filler. © 2015 Wiley Periodicals, Inc. *J. Appl. Polym. Sci.* 2015, 132, 42237.

**KEYWORDS:** composites; mechanical properties; recycling; thermal properties

Received 18 December 2014; accepted 17 March 2015

DOI: 10.1002/app.42237

### INTRODUCTION

Thermoplastics such as polyethylenes [PEs: high-density polyethylene (HDPE), low-density polyethylene (LDPE), and linear low density polyethylene (LLDPE)] and polypropylene (PP) constitute nearly 60–70% of the polymer waste and the remaining include polystyrene (PS) (approx. 10–15%), poly vinyl chloride (PVC) (approx. 15%) along with small quantities of polyethylene terephthalate (PET) (approx. 5%). PEs and PP constitute the major fraction of the polymer waste stream in India<sup>1</sup> and when disposed in land fills manifest a formidable threat to the environment because of their nonbiodegradable nature. Recycling of these is preferable over many other thermoplastics due to its lower melting point and ease in processing on conventional plastic processing equipment at a lower temperature and the process is quite economical.<sup>2</sup> However, recycling is usually accompanied by degradation and deterioration of their technical properties. Hence, recovery of some of its properties can be achieved by cross-linking, addition of fillers either particulate or fibrous, and modifying it to improve their property spectrum.

Biocomposites or natural fiber composites are composed of biodegradable natural fibers as reinforcement and biodegradable or nonbiodegradable polymers as matrix. They can be used as an alternative to glass fiber-reinforced polymer composites in automotive and construction industries that can be environmentally compatible.<sup>3</sup> They have also found applications in furniture and packaging industries.<sup>4</sup> The mechanical properties of natural fibers are much lower than those of glass fibers, but, their specific properties, especially stiffness, are comparable to those of glass fibers. They are 50% lighter than glass, and in general much cheaper.<sup>5</sup> Natural fiber-reinforced polymer (thermoplastic, thermosets, and rubber) composites have tremendous advantages over the conventional materials in the scientific world. They have gained vast popularity despite their high cost in high-performance products that need to be light weight yet strong to overtake harsh loadings.

Natural fibers are common industrial by-product that offers a great potential as reinforcing agent in recycled PEs in forming biocomposite materials. Some exclusive studies on the recycled HDPE (RHDPE)/natural fiber composites give us knowledge on

their dynamic properties to be useful in various areas. Lei *et al.*<sup>6</sup> have suggested that maleated PE (MAPE), carboxylated polyethylene, and titanium-derived mixture improve the compatibility between the bagasse fiber and RHDPE. The modulus and impact strength of the composites have maxima with MAPE content increase. Cui *et al.*<sup>7</sup> have obtained improvement in the mechanical properties of wood fiber/post consumer HDPE composites by addition of coupling agent (MAPP). Yao *et al.*<sup>8</sup> have described that both virgin and RHDPE/rice straw fiber composites have comparable mechanical properties with those of wood composites and they suggested rice straw fiber to be a suitable filler in recycled plastics. Favaro *et al.*<sup>9</sup> have observed improved flexural and impact properties from the composites prepared with modified sisal fibers and unmodified postconsumer HDPE matrix. Oza *et al.*<sup>10</sup> have observed that chemical treatment of hemp fibers improve the flexural strength of RHDPE/hemp fiber composites. Samariha *et al.*<sup>11</sup> have found that thickness swelling and water absorption increase with the increase in bagasse fiber content in RHDPE and Aht-Ong *et al.*<sup>12</sup> have suggested that PE-graft-maleic anhydride (PE-GMA) compatibilizer can improve the properties of the composites prepared from cellulose fiber (cotton waste fabric) and recycled PE. Some of our earlier publications<sup>13,14</sup> also reflect the beneficial properties obtained by the formation of composites using synthetic fibers (short PET and glass) as reinforcement in waste PE collected from municipal solid waste. The composites obtained are cost effective and can be useful for various construction purposes.

Coir fiber (CF) is the cheapest lignocellulosic natural fiber obtained from the fibrous mesocarp of coconuts, the fruit of coconut tree (*Cocos nucifera*). It is estimated that India and Srilanka account for nearly 90% of the world's coir production. Coir is a hard fiber, highly durable, relatively waterproof and has high abrasion resistance. Its efficiency as reinforcement in polymeric matrices is gaining vast importance. Njoku *et al.*<sup>15</sup> found out that environment friendly biodegradable composites having good strength and modulus can be produced with alkali treatment as well as fiber content variation in the CF reinforced cashew nut shell liquid-based biopolymer. Rao *et al.*<sup>16</sup> found out that both the treated and untreated coir can be successfully utilized to produce composite for value added products and increase in coir loading increased the wear resistance of CF-reinforced epoxy composites. Ayrilmis *et al.*<sup>17</sup> suggested that CF can be a partial replacement for heavier and costlier glass fibers and they obtained an increase in tensile strength, flexural strength, and modulus of elasticity for CF-reinforced PP composites. Karthikeyan and Balamurugan<sup>18</sup> found out that the impact strength of CF-reinforced epoxy composites improved with alkali treatment of fibers. Hussain *et al.*<sup>19</sup> studied the mechanical behavior of green CF-reinforced HDPE composites and observed improvement in the tensile, flexural, and impact strengths with variations in fiber length and volume fractions. Nam *et al.*<sup>20</sup> studied the mechanical properties of alkali-treated CF/poly (butylene succinate) composites and obtained an increase of tensile strength by 54.5%, tensile modulus by 141.9%, flexural strength by 45.7%, and flexural modulus by 97.4% compared to those of pure resin. Bettini *et al.*<sup>21</sup> investigated the use of CF as alternative reinforcement in PP and they obtained an increase in tensile strength, impact strength, and elastic modulus with decrease in elongation at break in pres-

ence of PP-g-MA. Wambua *et al.*<sup>5</sup> studied the effect of various natural fibers (sisal, kenaf, hemp, jute, and coir) as reinforcement in PP matrix. They suggested that the CF-reinforced composites displayed the lowest mechanical properties, but higher impact strength in comparison with other fibers. Fernandes *et al.*<sup>22</sup> studied the composites prepared from HDPE/cork powder/short CF and they obtained an increase in elastic modulus and tensile strength. Bhagat *et al.*<sup>23</sup> studied the mechanical properties and water absorption behavior of coir/glass fiber-reinforced epoxy-based hybrid composites and they observed an improvement in flexural strength (15 mm fiber length) and hardness (20 mm fiber length) of the composites at 10 wt % fiber loading. They also observed a minimum water absorption rate in the composites at 5 wt % fiber loading and at 5 mm fiber length. Zainudin *et al.*<sup>24</sup> studied the mechanical and morphological properties of coir/oil palm empty fruit bunch fibers-reinforced PP hybrid composites and they obtained an enhancement in the mechanical properties. They also suggested that the hybrid biocomposite material produced could be used to produce components like rear mirrors' holder and window levers, fan blades, mallet, or gavel.

Fly ash cenospheres (FACS) are small proportion of the pulverized fuel ash produced from the combustion of coal in power stations. They are unique free-flowing powders composed of hard-shelled, hollow, minute spheres consisting of silica, iron, and alumina. They have ultra low density, low thermal conductivity, high particle strength, resistant to acids, and low water absorption characteristics. These features suggest its use as a good candidate material (filler) in various matrices. Deepthi *et al.*<sup>25</sup> reported that silane coupling agent treatment of FACS and HDPE-g-dibutyl maleate as compatibilizer helps in improving the mechanical properties and thermal stability of the HDPE/FA composites. Chand *et al.*<sup>26</sup> observed excellent compatibility between the FACS and HDPE matrix by modification of FACS surface using silane treatment that resulted in considerable improvement in the impact strength and sensitivity of the composites which ultimately translated into better wear performance of composites even in severe abrasive conditions. The effect of silane coupling agent in FA-filled WPE/reclaim rubber blend<sup>27</sup> was evaluated in an earlier study by us and improvements in the tensile strength, flexural strength, flexural modulus, impact strength, and hardness of the blend composites was obtained. Recent studies<sup>28,29</sup> by us have suggested that use of FA as filler in WPE and HDPE matrices gave an enhancement in mechanical, thermal, and dynamic mechanical properties of the resulting composites with various modifications and this can be a good solution toward reduction of environmental pollution.

The effects of FACS on the detailed mechanical and physical characteristics of a natural fiber/recycled polymer composite have not been yet reported. However, there exist some literatures that indicate that the introduction of FA in the fiber/polymer system can be satisfactory for enhancing the mechanical properties. Kulkarni *et al.*<sup>30</sup> observed a better compressive strength and lowered density along with cost with the use of inexpensive FA in the E-glass fiber/epoxy system. They suggested an economically and engineering viable system to be obtained that could be considered for further development.

**Table I.** Physical and Chemical Properties of CF<sup>5,34</sup>

Property	Values
Density (g/cm <sup>3</sup> )	1.25
Tensile strength (MPa)	220
E-Modulus (GPa)	6
Elongation at break (%)	15–25
Moisture absorption (%)	10
Cellulose (wt %)	36–43
Lignin (wt %)	41–45
Hemicellulose (wt %)	10–20

Saxena *et al.*<sup>31</sup> obtained better physical, chemical, mechanical, weathering, and fire resistance properties than conventional materials like wood and wood substitute by using FA as filler in jute/sisal-reinforced polyester resin composites. They suggested that the developed composite system can be used for a number of applications like partitioning, false ceiling, roofings, panels, floorings, wall tiles, furniture, etc. Subham and Tiwari<sup>32</sup> studied the mechanical properties of FA-filled E-glass fiber/epoxy composites by varying FA concentrations and modifying the FA surface by  $\gamma$ -amino propyl triethoxy silane coupling agent. With surface modification of FA, the tensile and impact strength showed improvement resulting in good interfacial bonding and lower damping capability.

In this investigation, an effort has been made to evaluate the performance characteristics of RHDPE/CF-reinforced composites filled with FACS. MA-g-HDPE has been used as the coupling agent to improve the interfacial bonding between the fibers and RHDPE matrix. Variation in mechanical properties of RHDPE/CF composites as a function of FACS loading has been evaluated. The composite samples were subjected to dynamic mechanical analysis (DMA) measurements to evaluate the stiffness and damping properties under specific periodic stress. The fractured surface and interfacial adhesion morphology of the composites were also observed using scanning electron microscopy (SEM). Thermal stability of the samples has been studied using differential scanning calorimetry (DSC) and thermogravimetric analysis (TGA) thermograms. Water absorption and aging behavior were also investigated to evaluate the extent of mechanical degradation in the composites with aging.

## EXPERIMENTAL

### Materials

RHDPE was obtained from Sneha plastics, Hyderabad, India and was used as the base polymer matrix material. It was found to have an MFI of 0.84 g/10 min and density of 0.950 g/cc. Brown CF procured from Sri Srinivasa coir products, Hyderabad, India, was used as a reinforcing agent. The physical and chemical properties of CF are represented in Table I. MA-g-HDPE (OPTIM E-156) having MFI: 4.5 g/10 min and density: 0.954 g/cc was procured from M/s Pluss Polymers, India and has been used as a compatibilizer. FACS (grade: 5–150  $\mu$ m) was procured from Swift Services, Secunderabad. The average particle size of FACS used in the experiment was found to be 125

$\mu$ m, as shown in Figure 1. The assorted shape and size of the same was identified by SEM analysis, as shown in Figure 2. The FACS particles are mainly spherical in shape with relatively smooth surfaces having average particle density of 0.6–0.8 g/cc and their chemical composition being Al<sub>2</sub>O<sub>3</sub> (27–33%), SiO<sub>2</sub> (55–65%), and Fe<sub>2</sub>O<sub>3</sub> (6%).

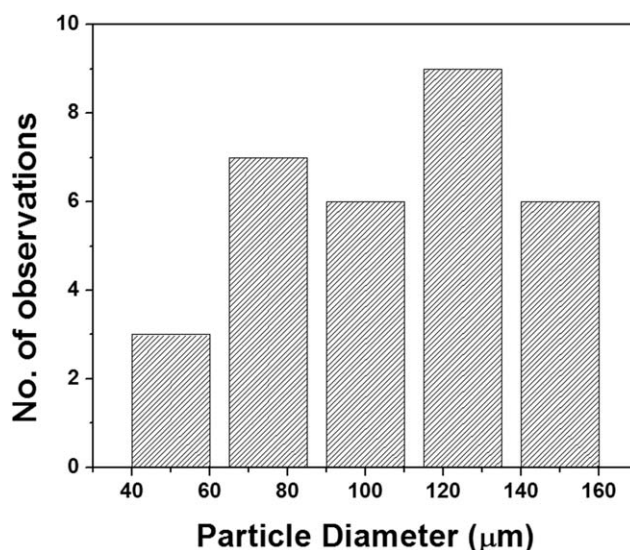
### Preparation of Biocomposites

The fibers were detergent washed and dried in vacuum oven at 70°C for 24 h before composite preparation. To ensure easy blending of the fibers with the RHDPE matrix, these detergent-washed fibers (untreated) were cut into a fiber length of  $\sim$ 6 mm manually.

Prior to compounding the ingredients, RHDPE, detergent-washed CF at different weight percents (10, 20, 30, and 40 wt %), MA-g-HDPE (1, 3, and 5 wt %), and FACS (2.5, 5, 7.5, and 10 wt %) were pre-dried in a vacuum oven.

In the first stage, RHDPE/CF at different weight percents of fiber (10, 20, 30, and 40 wt %) was compounded in an inter-meshing counter rotating JSW-twin-screw extruder (PR/EX/02, Japan). The process was carried out at a screw speed of 150 rpm and temperature range of 140, 150, 160, 170, and 180°C from the feed to die zone, respectively. The extrudates were cooled in water at room temperature, granulated in a pelletizer (HJC D75, Korea) and dried at 105°C for 4 h to eliminate residual humidity before injection molding. The dried granules were taken for preparation of mechanical (tensile, flexural, izod impact, and hardness) test specimens; according to ASTM D standards using an automatic injection molding machine (Kloner Windsor (P) Ltd., India, PR/AIM/02) at 190°C and injection pressure of 65 psi having a clamping force of 130 tons.

In the second stage, MA-g-HDPE at different weight percents (1, 3, and 5 wt %) was compounded with RHDPE/CF composites (30 wt % CF loading). Subsequently, these mixtures were injection molded to prepare required mechanical test samples. Finally, based on the weight of RHDPE, the FACS content was

**Figure 1.** Average particle size of FACS.

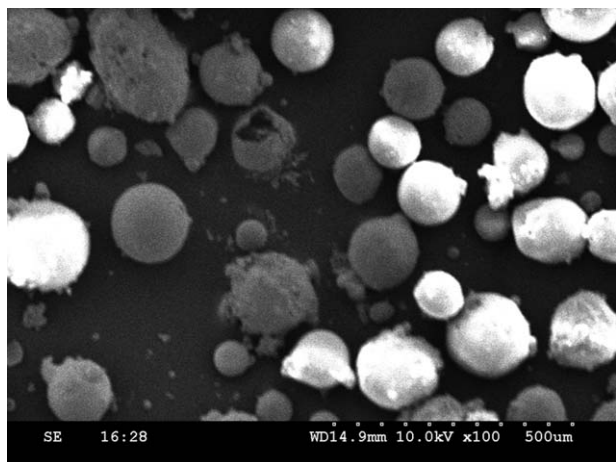


**Figure 2.** SEM micrograph of FACS particles.

varied (2.5, 5, 7.5, and 10 wt %) and the compounding was done at fixed loading levels of 30 wt % CF with 1 wt % MA-g-HDPE, respectively, to form RHDPE/CF/MA-g-HDPE/FACS composites. The mechanical test samples were prepared by injection molding as mentioned above.

#### Mechanical Testing

Tensile properties (tensile strength, tensile modulus, and elongation at break) of the biocomposites were measured as per ASTM D638 (standard test method for tensile properties of plastics) with gauge length of 60 mm, at a cross-head speed of 10 mm/min by using Universal Testing Machine (AGS-10 KNG, Shimadzu).

Flexural properties (flexural strength and modulus) were measured as per ASTM D790 (standard test method for flexural properties of unreinforced and reinforced plastics and electrical insulating materials) with gauge length of 60 mm, at a cross-head speed of 1.3 mm/min using the same Universal Testing Machine (AGS-10 KNG, Shimadzu).

Notched izod impact strength of the composite specimens was evaluated using an Impactometer (Tinius Olsen, USA) as per ASTM D256 (standard test method for determining the izod pendulum impact resistance of plastics) with a notch depth of 2.54 mm and notch angle of 45° using a 7 J hammer.

The shore D hardness values of the individual composites was determined according to ASTM D2240 (standard test method for rubber property, Durometer hardness) in a Shore D Hardness Tester (RR-12). Hardness is generally used to describe resistance of material to surface indentation, scratching, or marring. The measurements were carried out 15 s after the durometer tip had touched the sample.

Tests for determination of mechanical properties were carried out in a standard temperature of  $23 \pm 2^\circ\text{C}$  and  $50 \pm 2\%$  RH. The data reported are from the average of six specimens for each test. Corresponding standard deviations have also been reported.

#### Statistical Analysis

All mechanical data were statistically analyzed. The mechanical properties of the RHDPE/CF, RHDPE/CF/MA-g-HDPE, and RHDPE/CF/MA-g-HDPE/FACS composites were statistically

analyzed using *t*-test; *p* values  $<0.05$  were considered to be significant.

#### Thermal Properties

The melting, crystallization, and thermal stability of RHDPE and the composites with fiber and FACS were studied using DSC (TA Instruments, DSCQ100) and TGA (TA Instruments, TGAQ500), respectively.

DSC analysis was carried out using 5–10 mg of the samples at a scanning rate of  $20^\circ\text{C}/\text{min}$  and at a temperature of  $30\text{--}200^\circ\text{C}$  under nitrogen atmosphere. Subsequently, the samples were held at  $200^\circ\text{C}$  for 1 min and then cooled to  $30^\circ\text{C}$  at the same rate and was again reheated from 30 to  $200^\circ\text{C}$ . Corresponding melting temperature, heat of fusion, and crystallization temperature were recorded.

The thermal stability of the CF, RHDPE, and the composites was determined using TGA with samples of  $\leq 5$  mg weight and scanned from 40 to  $600^\circ\text{C}$  at a heating rate of  $20^\circ\text{C}/\text{min}$  under nitrogen atmosphere. The initial, final, and maximum degradation temperature and corresponding percentage weight loss for the samples were noted.

#### Water Absorption Test

Water absorption test of RHDPE/CF and RHDPE/CF/FACS composites was performed as per ASTM D570 (standard test method for water absorption of plastics). Specimens were dried at  $80^\circ\text{C}$  in a vacuum oven until a constant weight was attained. Subsequently, they were immersed in water in a thermo stated stainless-steel water bath at  $30^\circ\text{C}$ . Weight gain was recorded by periodic removal of the specimens from the water bath and weighing on a balance with a precision of 1 mg. The percentage gain at any time as a result of moisture absorption was determined.

#### Scanning Electron Microscopy

The SEM of tensile fractured composite specimens was carried out using Hitachi-S520 (Oxford Link-SEM Model, Japan). The samples were sputtered with gold and were dried for half an hour at  $70^\circ\text{C}$  in vacuum, before study.

#### Dynamic Mechanical Properties

The dynamic mechanical behavior of the samples was studied using dynamic mechanical analyzer (TA Instruments, DMAQ800). The experiments were carried out a fixed frequency of 1 Hz and at a heating rate of  $5^\circ\text{C}/\text{min}$ . The tests were conducted in a temperature range of  $-100$  to  $+100^\circ\text{C}$  using specimen of dimensions  $55 \times 10 \times 3$  mm.

## RESULTS AND DISCUSSION

### Mechanical Properties

**Effect of CF Loading on the Mechanical Properties of RHDPE/CF Composites.** The mechanical properties of RHDPE/CF composites at variable weight percentage of CF (10–30 wt %) are represented in Table II. It was observed that the composites prepared using CF loading of 40 wt % was difficult to process in the JSW twin-screw extruder. This may be probably due to improper wetting of the fibers within the RHDPE matrix which means the RHDPE content is not sufficient to wet all the fiber surfaces leading to poor interfacial adhesion, in turn difficulty

**Table II.** Mechanical Properties of RHDPE/CF, MA-g-HDPE Compatibilized RHDPE/CF and RHDPE/CF/FACS Composites

Sample	Tensile strength (MPa)	Tensile modulus (MPa)	Elong. at break (%)	Flexural strength (MPa)	Flexural modulus (MPa)	Izod impact strength (kJ/m <sup>2</sup> )	Hardness Shore D
RHDPE	25.51 (1.59)	146.34 (39.76)	128.02 (41.68)	25.08 (0.43)	154.03 (4.95)	22.43 (3.09)	60
RHDPE/CF (90/10)	24.87 (1.52)	173.99 (14.93)	37.52* (9.10)	26.33* (0.23)	173.93* (2.37)	17.38* (2.50)	62
RHDPE/CF (80/20)	24.92 (0.34)	209.96* (23.44)	17.51* (3.50)	26.95* (0.44)	190.33* (3.80)	16.30* (2.48)	64
RHDPE/CF (70/30)	23.21* (1.67)	360.84* (39.82)	8.95* (1.53)	29.02* (0.50)	276.42* (17.18)	13.83* (0.56)	70
RHDPE/CF/ MA-g-HDPE (69/30/1)	24.64 (1.21)	464.41* (57.07)	6.51* (1.29)	32.54* (1.53)	303.98 (34.41)	3.46* (0.13)	76
RHDPE/CF/ MA-g-HDPE (67/30/3)	22.06 (0.76)	354.12 (30.79)	13.6* (1.91)	30.97* (0.71)	298.60* (9.98)	3.69* (0.29)	74
RHDPE/CF/ MA-g-HDPE (65/30/5)	22.63 (0.67)	323.31 (42.86)	15.69* (3.39)	29.90* (0.51)	275.95 (6.35)	3.61* (0.20)	72
RHDPE/CF/ MA-g-HDPE/ FACS (66.5/30/1/2.5)	18.47* (0.27)	317.65* (35.96)	13.27* (0.74)	26.84* (0.59)	333.14 (18.98)	4.60* (0.42)	75
RHDPE/CF/ MA-g-HDPE/ FACS (64/30/1/5)	18.69* (0.54)	352.85* (30.66)	9.35* (1.22)	26.24* (0.85)	343.12* (14.07)	4.13* (0.42)	77
RHDPE/CF/ MA-g-HDPE/ FACS (61.5/30/1/7.5)	21.09* (0.75)	408.05 (63.71)	6.49 (1.30)	27.81* (0.82)	393.50* (57.87)	4.05 (0.58)	82
RHDPE/CF/ MA-g-HDPE/ FACS (59/30/1/10)	16.24* (1.63)	267.28* (15.78)	12.38* (2.51)	25.04* (0.48)	326.01 (31.15)	3.69 (0.20)	80

Values in parenthesis represent standard deviations.

\* $p < 0.05$ .

in processing. Thus in this case, CF loading up to 30 wt % in the RHDPE matrix was taken into account and the detail mechanical properties were studied thereof.

The tensile strength of RHDPE/CF composites with increase in fiber content are shown in Table II. Tensile strength is basically the ability of a material to resist breaking under tensile stress and is an important and widely measured property of materials used in structural applications. The force per unit area (MPa or psi) required to break a material in such a manner is the ultimate tensile strength or strength at break. Tensile strength of any composite depends on the chemical composition of the fiber and its internal structure. No significant difference was observed in the values of tensile strength with increase in CF content up to 20 wt % in comparison with RHDPE. The tensile strength of the composites decreased marginally by 9% with an increase in the CF content to 30 wt % (Table II). In this case, it is found that the tensile strength of RHDPE is 25.51 MPa ( $\pm 1.59$ ) and at 30 wt % CF loading, the tensile strength decreases to 23.21 MPa ( $\pm 1.67$ ). Cellulose content plays an important role in the tensile strength of natural-fiber-filled composites because cellulose chains have high resistance in tension.<sup>5,17</sup> In RHDPE/CF composites, the decrease in the tensile strength owes to the lower cellulose content of CF as compared to other natural fibers. Contrary results were obtained by Njoku *et al.*<sup>15</sup> in the case of CF/CNSL composites where they observed an increase in the tensile strength values with increase in CF

loading up to 30 wt %. However, a similar decrease in the tensile strength values of the composites were observed by Lei *et al.*<sup>6</sup> for RHDPE/bagasse fiber, Yao *et al.*<sup>8</sup> for RHDPE/rice-straw fiber, Favaro *et al.*<sup>9</sup> for RHDPE/sisal fiber, and Nourbakhsh *et al.*<sup>34</sup> for RHDPE/poplar fiber composites. They explained that the decrease in the tensile strength values of the RHDPE matrix with the incorporation of these natural fibers owed to the dewetting effect. In the fiber/matrix boundary region, stress concentrates around the reinforcement particle resulting in weak fiber–matrix interaction.

The tensile modulus value of the composites increased significantly ( $p < 0.05$ ) by 15% from 146.34 MPa ( $\pm 39.76$ ) to 360.84 MPa ( $\pm 39.82$ ) when the CF content increased from 10 to 30 wt % (Table II) in comparison with the RHDPE matrix. Tensile modulus is basically the measure of stiffness of a material. The observations from Table II clearly indicated that increasing the CF content significantly improved the stiffness of the RHDPE/CF composites. This increase in modulus of the RHDPE/CF composite with the increase in CF content can be attributed to the fact that the CF are stronger, stiffer, and capable of adhering to the RHDPE matrix enabling load transfer from the matrix to the fibers through the fiber/matrix interface.<sup>15,17</sup> A significant increase in the tensile modulus values was also observed by Favaro *et al.*<sup>9</sup> in RHDPE/sisal fiber composites. The elongations at break of all the composites are shown in Table II. It is evident that there is a severe fall in the elongation with the

incorporation of CF in the RHDPE matrix implying reduction in ductility of the matrix. A significant decrease in the values of elongation at break was observed in the composites from 10 to 30 wt % loading of fiber. The decrease in elongation of the composites was explained by some researchers as a result of destruction of structural integrity with the loading of CF leading to reduction in the ductile nature of the resin.<sup>15,35</sup>

The flexural properties of the samples as a function of increasing CF are presented in Table II. It is observed from the table that unlike tensile strength of the composites that show a slight decrease with increasing fiber loading, the flexural strength increased significantly ( $p < 0.05$ ) for the RHDPE/CF composites. The flexural strength of RHDPE is 25.08 MPa ( $\pm 0.23$ ) and at 30 wt % CF content, it increased to 29.02 MPa ( $\pm 0.50$ ). Nearly, 16% increase in the flexural strength was observed with the incorporation of 30 wt % of CF. The improvement of the flexural strength up to 30 wt % fiber content could be attributed to the increased network system by the CF as it has high aspect ratio. This results in increased bending properties of the composites.<sup>34</sup> A significant increase ( $p < 0.05$ ) in flexural modulus was also observed with an increase in CF loading and is found to be 79% at 30 wt % loading of fiber (Table II). The flexural modulus in case of RHDPE is 154.03 MPa ( $\pm 4.95$ ), which increased to 276.42 MPa ( $\pm 17.18$ ) at 30 wt % CF loading. This observation suggests that increasing CF content significantly improves the stiffness of the samples. The moduli of natural fibers are comparatively higher than that of the thermoplastic matrix. The increased flexural modulus of the composite samples with increasing fiber content owes to the higher moduli of the natural fiber. The increase in flexural modulus suggests efficient stress transfer between the polymer and fiber. The increase in flexural modulus can also be due to the mobility of the amorphous region which becomes increasingly restrained owing to the presence of fibers that are stiffer than the polymer matrix.<sup>23</sup> The increase in the modulus suggests good dispersion of the CF in the RHDPE matrix. The increase in flexural strength and flexural modulus is due to the finely distributed CF in the matrix and further increase in CF loading leads to the fiber coagulation in the composite resulting in difficulty in processing of the composites.

Table II also represents the izod impact strength of RHDPE/CF composites. Incorporation of CF resulted in a significant decrease in the izod impact strength of the RHDPE matrix. Incorporation of 30 wt % CF resulted in a decrease in the impact strength of the RHDPE matrix from 22.43 ( $\pm 3.09$ ) to 13.83 ( $\pm 0.56$ ) kJ/m<sup>2</sup>. This decrease in the impact strength was due to the presence of CF in the composites, which reduced the energy absorbed by the composites. Agunsoye *et al.*<sup>35</sup> observed a decrease in impact energy of the PE composites with an increase in coconut shell particles content, where the sample with 25% volume fraction coconut shell particles in the matrix showed the lowest impact energy of 1.76 J. The impact properties determine the ability of a material to withstand an impact load and are basically the toughness of the material. The impact strength of the composites decreases as the fiber loading is increased. This reflects the reduction in energy absorption at the crack tip.<sup>36</sup> The poor bonding quality between the fiber and

the polymer matrix creates weak interfacial regions which will result in debonding and frictional pull out of fiber bundles. These failure mechanisms, which inhibit the ductile deformation and mobility of the matrix, will obviously lower the ability of the composite system to absorb energy during fracture propagation.<sup>35</sup> From the table, it is evident that the toughness of the composites decreases with increase in the CF loading. Similar decrease in impact strength of RHDPE with variation in fiber loading was observed by other researchers as well.<sup>6,8,37,38</sup>

The Shore D hardness values of the samples increased by 17% when the CF content increased from 10 to 30 wt % in the composite (Table II). This was consistent with previous studies.<sup>17,36</sup> The hardness value was determined by the penetration of the durometer indenter foot into the specimen. The results obtained give us an insight into the relative resistance to indentation of various composites. From the results obtained, it is observed that the hardness values of the composites increases with increase in fiber loading and is the maximum at 30 wt % CF loading having a value of 70. This implies that the degree of resistance of the composite to indentation measured in shore durometer is high.<sup>39</sup> The improvement in the hardness values was due to the high lignin content of the CF. CF is a tough and stiffer fiber owing to the presence of high lignin content and this in turn acts as a force in increasing the stiffness of the composites.

**Effect of Compatibilizer (MA-g-HDPE) on the Mechanical Properties of RHDPE/CF Composites.** Addition of CF (10–30 wt %) into RHDPE matrix results in a decrease in the tensile strength, izod impact strength, and elongation at break values of the RHDPE/CF composites. However, a significant increase in tensile modulus, flexural strength, flexural modulus, and hardness values are observed with increase in CF loading. Hence, to study any further possibility of enhancement in the mechanical properties of the RHDPE/CF composites, MA-g-HDPE was used as a compatibilizing agent. From literature,<sup>40,41</sup> it is evident that MA-g-PE and MA-g-PP acts as a dispersing agent between the polar fibers and the nonpolar matrix resulting in improved interfacial adhesion. They contribute to enhanced stress transfer from the matrix to the fiber, in turn increasing the properties further. Composites prepared at 30 wt % of CF loading have been taken for compatibilization with MA-g-HDPE (1, 3, and 5 wt %) and the mechanical properties were studied in detail. Addition of MA-g-HDPE resulted in significant increase in the mechanical properties of RHDPE/CF composites, which is in agreement with the results observed by other researchers.<sup>6,42</sup>

The composites prepared at 30 wt % CF loading and 1 wt % MA-g-HDPE exhibited optimum mechanical strength (Table II). It was observed that the tensile strength of RHDPE/CF/MA-g-HDPE composites increased to 6% [23.21 ( $\pm 1.67$ ) to 24.64 ( $\pm 1.21$ ) MPa], tensile modulus to 29% [360.84 ( $\pm 39.82$ ) to 464.41 ( $\pm 57.07$ ) MPa], flexural strength to 12% [29.02 ( $\pm 0.50$ ) to 32.54 ( $\pm 1.53$ ) MPa], flexural modulus to 10% [276.42 ( $\pm 17.18$ ) to 303.98 ( $\pm 34.41$ ) MPa], and hardness (Shore D) to 9% [70 to 76], respectively, when compared with RHDPE/CF composites without MA-g-HDPE. However, the elongation at

break and izod impact strength of the composites decreased significantly with the incorporation of MA-g-HDPE in the RHDPE/CF composite system. A similar decrease in the values of impact strength in presence of compatibilizer was observed by Bettini *et al.*<sup>21</sup> in case of CF-reinforced PP composites suggesting that the amount of energy dissipated decreased, resulting in increased adhesion between the fibers and the matrix.

From statistical analysis, significant increase ( $p < 0.05$ ) in tensile modulus, flexural strength, and hardness values were found in the RHDPE/CF composites with the addition of only 1 wt % of MA-g-HDPE (Table II). The increase in the mechanical behavior of the composites with the addition of compatibilizer was explained by Biswal *et al.*<sup>40</sup> that the anhydride groups present in the compatibilizer reacts with the hydroxyl groups of the natural fibers forming an ester linkage at the interface. The high-molecular-weight MA-g-HDPE having more flexible PE chains can diffuse into the RHDPE/CF matrix leading to interchain entanglements, thereby contributing to the mechanical continuity of the system. This improves the fiber–matrix interface by reducing the void volume between the fibers and the matrix.<sup>13,34,43</sup> However, further increase in the MA-g-HDPE content to 3 and 5 wt % resulted in a decrease in the mechanical strength of the composites.

**Effect of FACS on the Mechanical Properties of RHDPE/CF/MA-g-HDPE Composites.** The RHDPE/CF/MA-g-HDPE composite samples at 30 wt % CF loading and 1 wt % MA-g-HDPE showed optimum mechanical properties. This composition has been taken for fabrication with FACS and for further characterization studies. The mechanical properties of RHDPE/CF/MA-g-HDPE composites containing different weight percentage of FACS (2.5, 5, 7.5, and 10 wt %) are depicted in Table II.

It was observed that the addition of FACS particles decreased the tensile strength of the composites (Table II). There was a significant decrease in the values of tensile strength when FACS content was increased from 2.5 to 5 wt %. However, there was a significant increase ( $p < 0.05$ ) in the tensile strength with an increase in FACS content to 7.5 wt %. The decrease in the values of tensile strength at 2.5 and 5 wt % FACS loading can be explained because of the dilution effect, i.e., the FACS amount is not sufficient to enhance the polymer–fiber matrix. Similar decrease in the values of tensile strength with increase in FA loading was observed by Subham and Tiwari<sup>32</sup> in case of Epoxy/glass fiber/FA composites. They explained this reduction was due to the voids formed at the FA–resin interface which act as stress risers when tensile load was applied onto the composites leading to decrease in stress bearing capacity. At 7.5 wt % FACS loading, the increase in the value of tensile strength was due to the effective dispersion of FACS in the RHDPE/CF matrix.<sup>29</sup> With further increase in the FACS content to 10 wt %, the value of tensile strength was decreased due to the phenomenon of agglomeration of the filler particles and also filler–filler interaction being more in comparison with the polymer–filler interaction, leading to a weak polymer/filler matrix.<sup>28</sup> The tensile modulus values also initially decreased with the FACS loading from 2.5 to 5 wt % followed with an increase at 7.5 wt %. With further increase

in the FACS loading to 10 wt %, the value of tensile modulus was decreased owing to the predominance of filler–filler interaction over polymer–filler interaction. The statistical analysis suggests that there was an increase in the values of tensile strength and modulus of the RHDPE/CF/FACS composite at 7.5 wt % of FACS, in comparison with the FACS loading at 2.5, 5, and 10 wt % loading. However, the values were comparatively less than that of RHDPE/CF/FACS composite with 0 wt % FACS loading. There was a significant decrease in the values of elongation at break with the increase in FACS loading. This decrease in the value of elongation at break with increase in filler loading owes to the rigid FACS particles,<sup>28</sup> which reduced the flexibility of the polymer/fiber matrix.

The flexural strength and modulus of the RHDPE/CF composites with variation in FACS loading from 2.5 to 10 wt % was measured. The flexural properties of composite samples are shown in Table II. The flexural strength and modulus of RHDPE/CF composites compatibilized with MA-g-HDPE at 0 wt % FACS loading were found to be 32.54 ( $\pm 1.53$ ) and 303.98 ( $\pm 34.41$ ) MPa, respectively. FACS incorporation significantly increased ( $p < 0.05$ ) the flexural modulus to 333.14 ( $\pm 18.98$ ) MPa and decreased the flexural strength to 26.84 ( $\pm 0.59$ ) MPa at only 2.5 wt % of FACS. The flexural strength decreased by 18% at 2.5 wt % FACS loading, 19% at 5 wt % FACS loading, 15% at 7.5 wt % FACS loading, and 23% at 10 wt % FACS loading in comparison with 0 wt % FACS loading. The decrease was less in case of 7.5 wt % FACS loading in comparison with the other loadings. Similar observation was obtained by Sengupta *et al.*<sup>44</sup> in case of recycled PP/FA composites with increase in FA loading. They suggested some possible mechanical anchorage between the filler and polymer matrix although there may not be much physical interaction between them. However, the rigidity of the RHDPE/CF composites were further improved with the addition of FACS. The modulus increased significantly ( $p < 0.05$ ) by 10, 13, 29, and 7% at 2.5, 5.0, 7.5, and 10 wt % FACS loading, respectively, in comparison to that without FACS. An increase in flexural modulus values indicated an enhancement in rigidity of the composites, especially in case of composites with 7.5 wt % FACS loading. Thus incorporation of filler increased the flexural modulus due to restriction in chain mobility which was more pronounced at 7.5 wt % FACS loading. This increase in modulus values with the addition of reinforcing filler owes to effective stress transfer from the matrix to the filler at the interface.<sup>45,46</sup> Thus a decrease in flexural strength along with an increase in flexural modulus was observed in the composites. Such increase in flexural modulus with decrease in flexural strength in polymer matrix on incorporation of filler has been reported earlier.<sup>47</sup>

The notched izod impact strength of the RHDPE/CF/MA-g-HDPE composites did not show any appreciable change with the incorporation of FACS (Table II). Similar observation in the impact property values was observed by Nourbakhsh *et al.*<sup>48</sup> in case of PP/bagasse fiber/nanoclay composites. It is due to the stiffening of the polymer chains. The presence of FACS particles makes the failure mode brittle and relatively less energy is absorbed by the composite having sound dispersoid/matrix bonding allowing less energy absorption and less impact

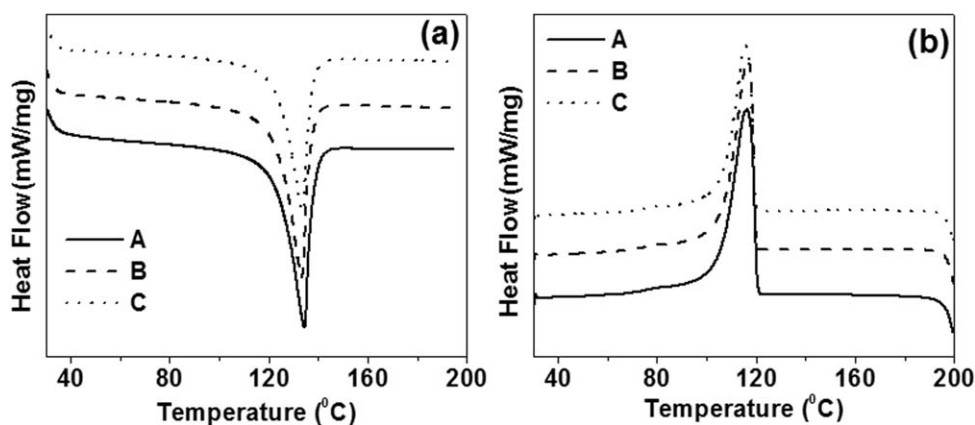


**Figure 3.** DSC (a) heating and (b) cooling curve of (A) RHDPE, (B) RHDPE/CF/MA-g-HDPE, and (C) RHDPE/CF/MA-g-HDPE/FACS composites.

strength values.<sup>33</sup> The shore D hardness values of the RHDPE/CF/MA-g-HDPE composites filled with FACS are shown in Table II. There was a significant increase in the hardness values with increase in FACS loading and was maximum at 7.5 wt %. Similar increase in hardness values with both FA and fibers as reinforcements was obtained by Patel *et al.* in case of carbon-FA/panox fiber composites.<sup>49</sup>

The mechanical findings were in agreement with the morphological interpretations from SEM as discussed in later section. At 7.5 wt % FACS loading, the RHDPE/CF/MA-g-HDPE composite had optimum tensile strength, tensile modulus, and flexural strength values with significant enhancement ( $p < 0.05$ ) in flexural modulus and hardness values suggesting that the incorporation of FACS was indeed beneficial in the cost reduction and remarkable utilization of the developed composite. Our results corroborates with the results of Saxena *et al.*<sup>33</sup> where they also obtained optimum mechanical strength values in case of polyester resin/jute fiber/FA and polyester resin/sisal fiber/FA composites. Such developed composite materials have potential to be cost- and energy-effective wood substitute for building applications.

### Thermal Properties

**Differential Scanning Calorimetry.** Figure 3(a,b) shows the heating and cooling curves of DSC analysis of RHDPE, RHDPE/CF/MA-g-HDPE composites along with RHDPE/CF/MA-g-HDPE/FACS composites. Melting point and crystallinity of all the samples were investigated using DSC curves and are shown in Table III. The melting temperature ( $T_m$ ) of the RHDPE and its composites with CF and FACS was taken as the maximum of the endothermic peak obtained from the second heating [Figure 3(a)], whereas the crystallization temperature ( $T_c$ ) was taken as the maximum of the exothermic peak from the cooling cycle [Figure 3(b)]. It was observed that the  $T_m$  of the RHDPE matrix decreased marginally with the incorporation of CF and FACS. This implies an improvement in the processing temperature of the RHDPE.<sup>8</sup>

Comparing the DSC cooling thermograms of RHDPE with respect to RHDPE/CF composite, it is observed that the  $T_c$  of RHDPE was about 116.25°C, with a degree of crystallinity,  $X_c$  of 53.58% (Table III). Incorporation of 1 wt % MA-g-HDPE in

RHDPE/CF composite results in significantly no change in  $T_c$  (116.82°C). This may be attributed to homogenous crystallization and the amount of the crystalline portion has the same order of magnitude as the initial material.<sup>50</sup> However, the degree of crystallinity,  $X_c$  decreased to 44.50% suggesting that presence of MA-g-HDPE reduced the perfection of RHDPE crystals. Addition of FACS to RHDPE/CF/MA-g-HDPE system showed a  $T_c$  of 116.04°C and degree of crystallinity of about 43.13%.

As observed from Table III, melting (or crystallization) enthalpy ( $\Delta H_f$ ) and  $X_c$  of RHDPE/CF/MA-g-HDPE composites decreased in comparison with the RHDPE matrix. This reduction is related to the transcrystalline region in which restrictions in the lateral direction of growth of spherulites are observed, resulting in a columnar layer.<sup>51</sup> The lower melting point and temperature of crystallinity as well as the differences in degree of crystallinity indicate that the crystallization process is affected, and crystals formed are small in size.<sup>40</sup> Lei *et al.*<sup>6</sup> also reported a lowered crystallinity level in the RHDPE/Bagasse fiber composites in presence of MA-g-PE suggesting an improvement in the compatibility and reduction of perfection of RHDPE crystals. In case of RHDPE/CF/MA-g-HDPE/FACS system, the heat of crystallization is decreased further indicating the interference of FACS in the crystalline packing of the RHDPE matrix and this shows an interaction between the component phases in the biocomposite.

The degree of crystallinity has been estimated using the following equation

**Table III.** Melting and Crystallization Behavior of RHDPE, MA-g-HDPE Compatibilized RHDPE/CF and RHDPE/CF/FACS Biocomposites

Sample	$T_m$ (°C)	$T_c$ (°C)	$\Delta H_f$ (J/g)	$X_c$ (%)
RHDPE	134.33	116.25	157.0	53.58
RHDPE/CF/ MA-g-HDPE	133.24	116.82	130.4	44.50
RHDPE/CF/ MA-g-HDPE/FACS	133.61	116.04	116.9	43.13



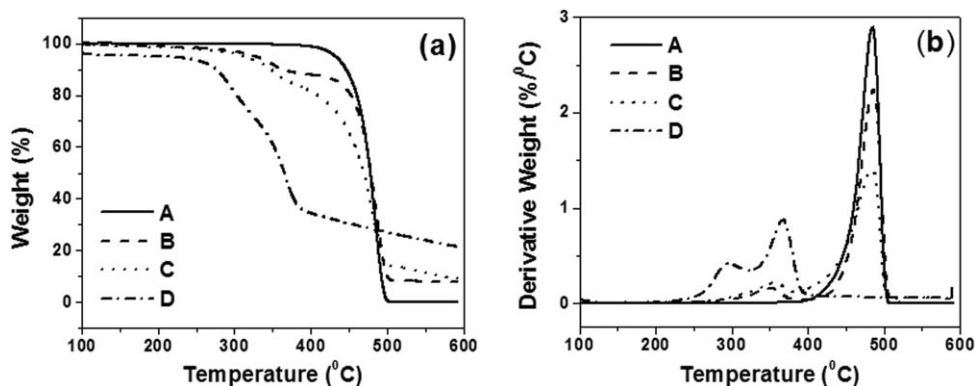


**Figure 4.** TGA thermographs of (a) weight loss and (b) derivative weight loss with temperature of (A) RHDPE, (B) RHDPE/CF/MA-g-HDPE, (C) RHDPE/CF/MA-g-HDPE/FACS, and (D) CF.

$$X_c(\%) = \Delta H_f \times 100 / \Delta H_{100\%} (1 - W_w)$$

where  $X_c$  is the percentage of crystallinity,  $\Delta H_f$  is the experimental melting heat of fusion,  $\Delta H_{100\%}$  is the heat of fusion of 100% crystalline HDPE (293 J/g),<sup>6</sup> and  $W_w$  is the weight fraction of FACS.

**Thermogravimetric Analysis.** The determination of thermal properties by TGA analysis is an important study in the development of biocomposites owing to the low thermal degradation of natural fibers. Degradation of the fibers and fillers during processing may have a detrimental effect upon the mechanical properties of the composites.<sup>41</sup> TGA and differential thermal analysis (DTA) curves of RHDPE and the composites (RHDPE/CF and RHDPE/CF/FACS compatibilized with MA-g-HDPE) are shown in Figure 4(a,b), respectively, and the properties are tabulated in Table IV.

The TGA curve [Figure 4(a)] of CF exhibits two main decomposition steps. The first one is in between 267 and 304°C, and the second one is in between 351 and 381°C. The initial moisture absorption in case of CF was not noticed in this case, which is probably due to detergent treatment of the fibers<sup>40</sup> that resulted in rough topology. The degradation of CF starts at 267°C with the decomposition of hemicellulose (267–304°C), followed by the decomposition of cellulose and lignin in the range of 351–381°C.<sup>52</sup> Above 381°C, the carbonization of fiber occurs with some mass loss, showing a residual mass of approximately 21.5% at the end of the process. In the case of RHDPE, it was

observed that its thermal decomposition showed a narrow temperature range with degradation in a single mass loss step (461–494°C). The maximum percentage of RHDPE was found to decompose at 484°C. The residual mass at the end of the analysis was about 0.1%.

From the DTA curves [Figure 4(b)], it was observed that the single major decomposition peak for RHDPE was from 461 to 494°C with a maximum peak ( $T_{max}$ ) at 484°C, while composites showed two major peaks. With the addition of CF, the final decomposition temperature increased from 494°C for RHDPE to 497°C for composites with 30 wt % CF and 1 wt % MA-g-HDPE. Hence the RHDPE/CF composites with MA-g-HDPE start to lose weight at higher temperatures compared to the RHDPE matrix. This apparent improvement in thermal stability of the composite could be attributed to the presence of MA-g-HDPE. MA-g-HDPE is able to bond with the hemicellulose in the CF, thus stabilizing its structure and improving the thermal stability of the composite.<sup>53</sup> The poor thermal stability of hemicelluloses and pectin in a composite can thus be overcome by the inclusion of a coupling agent.

For the RHDPE/CF composites prepared with 30 wt % of CF and 1 wt % MA-g-HDPE, a two-step degradation process was found. The first step is attributed to the decomposition of CF (312–364°C) and the second one corresponded to the decomposition of RHDPE matrix (463–497°C). The charred residue in this case was found to be 8.1%. In case of RHDPE/CF composites compatibilized with MA-g-HDPE and filled with FACS

**Table IV.** TGA Data of RHDPE, MA-g-HDPE Compatibilized RHDPE/CF and RHDPE/CF/FACS Biocomposites

Sample	Stage	Temperature range (°C)	$T_{max}$ (°C)	Residue (%)
RHDPE	First	461–494	484	0.1
RHDPE/CF/MA-g-HDPE	First	312–364	349	8.1
	Second	463–497	486	
RHDPE/CF/MA-g-HDPE/FACS	First	314–365	355	9.2
	Second	453–495	485	
CF	First	267–304	295	21.5
	Second	351–381	367	

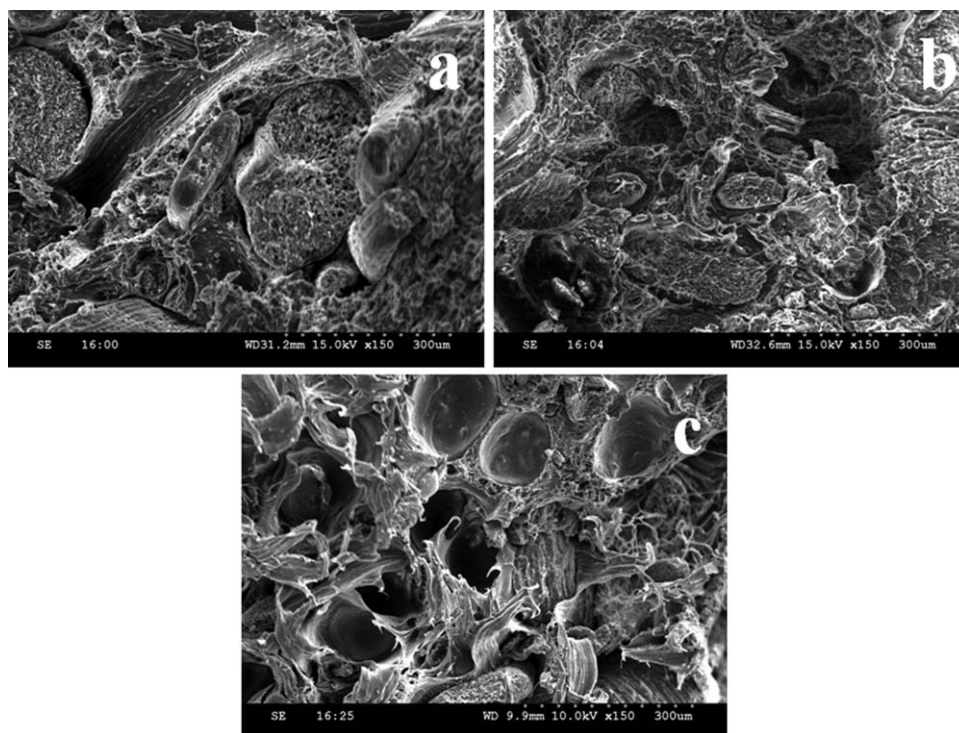


**Figure 5.** SEM micrographs of (a) RHDPE/CF, (b) RHPE/CF/MA-g-HDPE, and (c) RHDPE/CF/MA-g-HDPE/FACS composites.

(7.5 wt %), the thermal decomposition again occurs in two steps. The first one is in the range of 314–365°C (decomposition of CF) and the second one is in between 453 and 495°C (decomposition of RHDPE). The  $T_{\max}$  of CF is enhanced further, while that of RHDPE is found to be intermediate in the FACS-filled composite in comparison with the RHDPE and RHDPE/CF composites. In RHDPE/CF/MA-g-HDPE/FACS composites, the  $T_{\max}$  is 355°C in first stage and 485°C in second-stage degradation. The charred residue was found to be 9.2%. Thus it is clear that addition of CF enhances the thermal stability of the RHDPE/CF/MA-g-HDPE composites and with addition of FACS, the thermal stability attains an optimum. This optimum in thermal stability of the biocomposites (RHDPE/CF/MA-g-HDPE/FACS) is attributed to the organic/inorganic interaction between the polymer and filler as suggested by Biswal *et al.*<sup>40</sup> in case of PP/PALF/nanoclay composites. By comparing the thermal stability and weight loss with the RHDPE, it is observed that the weight loss at final decomposition temperature is increased for the FACS-filled biocomposite samples. The optimum thermal stability is attributed to interaction of base polymer and FACS surface through chemical linkage between compatibilizer and FACS, which in turn mediates the surface polarity of the FACS and the polymer/FACS interface. The FACS delays volatilization of the products generated at the temperature of carbon–carbon bond scission of the polymer matrix.

#### Scanning Electron Microscopy

The morphology of the tensile fractured surfaces of RHDPE/CF composites with and without MA-g-HDPE and RHDPE/CF/FACS composites with MA-g-HDPE is depicted in Figure 5(a–c). Figure 5(a) reveals fiber pullouts and gaps between the

RHDPE matrix and fiber in case of RHDPE/CF composites without MA-g-HDPE. This indicates poor interfacial adhesion and dewetting of the untreated fibers within the RHDPE matrix. The morphology so obtained was due to the large difference in the surface energies between the hydrophilic fibers and the hydrophobic matrix.<sup>40</sup> However, in presence of MA-g-HDPE compatibilizer, the fibers were well coated and embedded within the RHDPE matrix as shown in Figure 5(b). In this case, during tensile testing, fibers are pulled out together with the RHDPE matrix which suggests sufficient bonding as well as interfacial adhesion between RHDPE, CF, and MA-g-HDPE. This morphology resulted in improved mechanical properties of the composite system. Our observation from SEM was in concurrence with that of the fractured surfaces of RHDPE/bagasse fiber and RHDPE/pine fiber, where MA-g-HDPE as compatibilizer resulted in good dispersion and wetting of the fibers in the matrix producing strong interfacial adhesion and composite materials with satisfactory mechanical properties.<sup>6</sup> In the case of RHDPE/CF/FACS composite samples [Figure 5(c)], addition of FACS to RHDPE/CF composites in presence of MA-g-HDPE exhibited improved dispersion of CF within the RHDPE matrix with considerable reduction in the gaps between the fiber and the matrix. The FACS particles were encapsulated in the RHDPE/CF matrix resulting in less flaws and defects. Phenomenal morphological distinction was observed in the SEM micrographs of RHDPE/CF composite without MA-g-HDPE and RHDPE/CF, RHDPE/CF/FACS composites with MA-g-HDPE.

#### Water Absorption Test

The influence of CF and FACS on the water absorption values of RHDPE/CF composites and RHDPE/CF/FACS composites is shown in Figure 6. It is evident from the test results that there

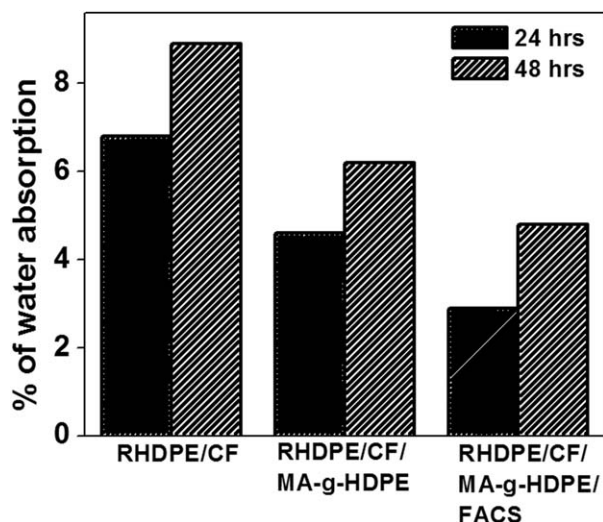


**Figure 6.** Water absorption characteristics of (Column 1) RHDPE/CF, (Column 2) RHDPE/CF/MA-g-HDPE, and (Column 3) RHDPE/CF/MA-g-HDPE/FACS.

is a linear increase in the water absorption in all the samples with increase in the immersion time. However, with the addition of MA-g-HDPE into the RHDPE/CF composites, the water absorption values are lowered, which is further lowered with the incorporation of FACS filler in the composite.

Literature studies reveal that the water resistance of the CF-reinforced thermoplastic composites is much better in comparison with other natural fibers like hemp, kenaf, jute, sisal, flax, and empty fruit bunch. This good water resistance of CF-reinforced thermoplastic matrix is due to the low cellulose and high lignin content of CF.<sup>17</sup> From Figure 6, it is observed that the RHDPE/CF composite sample exhibited a greater tendency of water absorption in comparison with the RHDPE/CF/MA-g-HDPE composite, which is due to the hydrophilic nature of CF. With the inclusion of MA-g-HDPE as compatibilizer in the RHDPE/CF composite system, the water absorption is decreased. MA-g-HDPE acts as a dispersing agent between the CF (polar part) and RHDPE matrix (nonpolar part) resulting in improved fiber/matrix bonding, in turn enhancing the water resistance capacity.<sup>34,54</sup> With the incorporation of FACS into the RHDPE/CF/MA-g-HDPE composites, the water absorption values decrease considerably. In the case of RHDPE/CF/FACS biocomposites, the presence of FACS creates longer diffusion paths resulting in less water absorption in comparison with the composites without FACS. The presence of FACS in the voids of the CF and RHDPE matrix prevents penetration of water into the deeper parts of the composite and the presence of MA-g-HDPE leads to better interaction and decrease in water absorption values. Biswal *et al.*<sup>40</sup> and Nourbaksh *et al.*<sup>48</sup> obtained similar reduction in the values of water absorption in hybrid composite systems (PP/natural fiber/nanoclay).

#### Dynamic Mechanical Analysis

The dynamic mechanical properties of the RHDPE, RHDPE/CF, and RHDPE/CF/FACS composites compatibilized with MA-g-HDPE were investigated to get a clear idea about the matrix/

fiber–filler interactions. The DMA curves of the composites with increase in temperature are shown in Figure 7(a–c).

**Storage Modulus ( $E'$ ).** The elastic component,  $E'$ , is a measure of load-bearing capacity of a material and is analogous to flexural modulus, determined in accordance with ASTM D790.<sup>47,53</sup> The variation of storage modulus as a function of temperature for different samples is graphically represented in Figure 7(a). It is evident that by addition of CF, the modulus of the RHDPE matrix is increased. This behavior is primarily attributed to the reinforcing effect imparted by the fibers that allowed a greater degree of stress transfer at the interface resulting in increase in

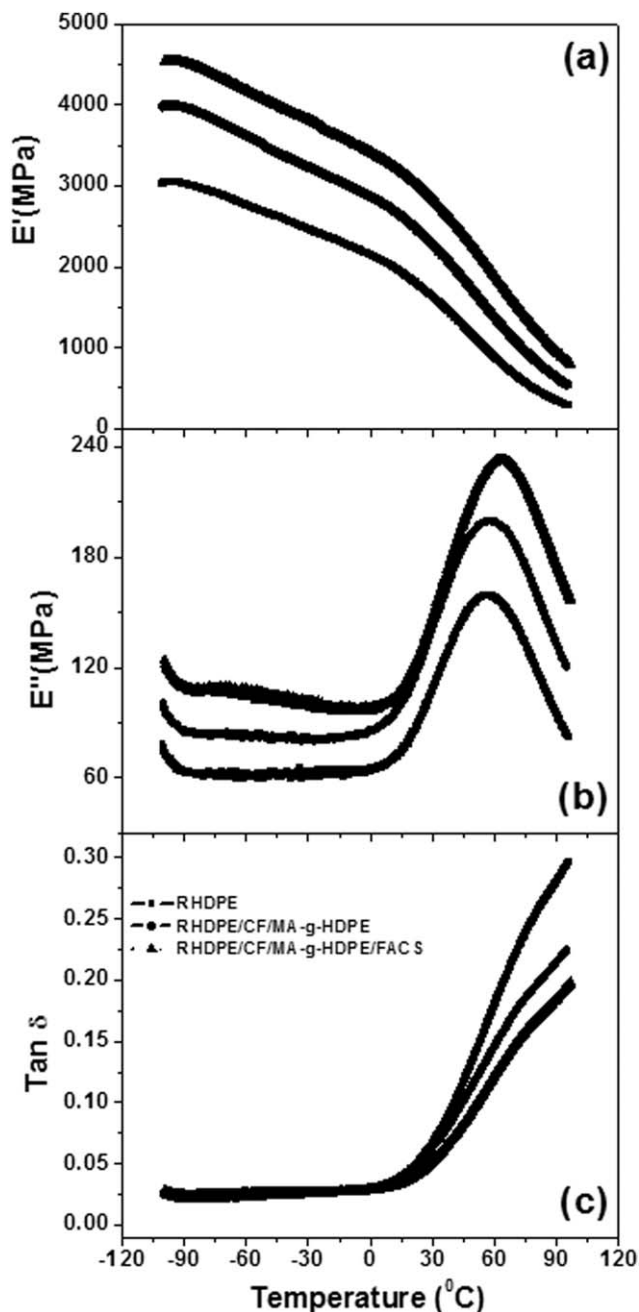


**Figure 7.** (a) Storage modulus, (b) loss modulus, and (c) loss tangent of RHDPE biocomposites with respect to RHDPE.

the stiffness.<sup>55</sup> A comparative higher magnitude of  $E'$  was observed with the RHDPE/CF composites filled with FACS over the entire range of temperature, thus showing improved dispersion of the FACS within the fiber–resin matrix. These observations were in agreement with the flexural modulus values. In all the samples, the storage modulus decreased with the increase in temperature. In case of RHDPE, the storage modulus drops steeply on increasing the temperature because of increased segmental mobility of the polymer chains. However, incorporation of CF and FACS reduces the rate of fall of the matrix modulus with temperature, thus indicating higher stability of RHDPE in the FACS-filled RHDPE/CF/MA-g-HDPE composite system.

For RHDPE, the highest storage modulus value was found to be 3131.62 MPa, transition temperature from loss modulus peak [Figure 7(b)] was 57.52°C, and the damping value [Figure 7(c)] at the transition temperature was 0.18. The variation of the storage modulus as a function of temperature is shown in Figure 7(a). CF reinforcement did increase the storage modulus value to 4086.84 MPa and FACS addition enhanced it further to 4645.55 MPa, indicating an improvement in interfacial bonding and stiffness of the composites.<sup>56</sup>

**Loss Modulus ( $E''$ ).** From literature, it is evident that DMA of PE exhibits three peaks, i.e.,  $\alpha'$ ,  $\beta$ , and  $\gamma$  transitions when loss modulus is plotted against temperature. Of these, the  $\gamma$  transition occurs between  $-150$  and  $-120^\circ\text{C}$ ,  $\beta$  relaxation occurs between  $-30$  and  $10^\circ\text{C}$ , and  $\alpha'$  transition is usually found between  $30$  and  $60^\circ\text{C}$ .<sup>57,58</sup> Of these transitions,  $\alpha'$  transition is assumed to be due to molecular motion in the crystalline region which occurs much below the melting temperature of the highly crystalline polymers, for example, HDPE and isotactic PP. The  $\beta$  relaxation peak that occurs at a lower temperature is a weak secondary relaxation peak occurring due to side-chain motion of ester or alkyl groups attached to the main chain. This  $\beta$  relaxation peak is very conspicuous in LDPE and HDPE. The  $\gamma$  relaxation occurs at a much lower temperature and is assumed to be due to small short-range motion of 3–4 methylene groups in a row in the amorphous zone and is also corroborated with crankshaft mechanism of the polymers. However, in HDPE and LDPE, the  $\gamma$  relaxation temperature is considered to be the glass transition temperature of the polymer which is difficult to identify.<sup>59</sup>

In this study,  $\alpha'$  relaxation phenomenon of RHDPE, RHDPE/CF, and RHDPE/CF/FACS composites with MA-g-HDPE has been investigated from loss modulus ( $E''$  curves) represented in Figure 7(b). The loss modulus curves of RHDPE as well as the biocomposites with CF and FACS exhibited a single prominent peak at 30–60°C which can be attributed to the  $\alpha'$  transition temperature. From the figure, this  $\alpha'$  transition temperature is significantly shifted to higher temperature in case of RHDPE/CF/MA-g-HDPE and RHDPE/CF/MA-g-HDPE/FACS composites in comparison with RHDPE. In the case of RHDPE, the maxima of the  $\alpha'$  peak is obtained at a temperature of 57.52°C. In the case of RHDPE/CF composites, the  $\alpha'$  transition peak is shifted to higher temperature, i.e., 58.50°C. This shift to higher temperature although marginally is primarily attributed to the restriction in the mobility of the polymer chains in the crystal-

line phase so that more energy is required for the transition to occur. Further with the addition of FACS, an increase in the  $\alpha'$  transition peak temperature to 64.56°C of RHDPE/CF composites was observed which indicates a genuine interface. This type of loss modulus spectra have been reported earlier in case of wood flour filled HDPE composites,<sup>60</sup> where a single prominent transition was seen due to the presence of filler that results in inhibition of relaxation process resulting in decrease in the chain mobility in the crystallites.

The loss modulus values at the  $\alpha'$  transition temperature increased for RHDPE/CF and RHDPE/CF/FACS composites with MA-g-HDPE as observed in Figure 7(b). The loss modulus was 163.71 MPa in case of RHDPE, which significantly increased to 203.85 MPa in RHDPE/CF/MA-g-HDPE and 238.26 MPa in case of RHDPE/CF/MA-g-HDPE/FACS composites. This increase in the loss modulus value of the composites with FACS owes to maximum viscous dissipation<sup>47</sup> in comparison with the RHDPE matrix. This has been reflected in the flexural strength measurements as reported in our earlier section.

**Loss Tangent ( $\tan \delta$ ).** The variation of the  $\tan \delta$  as a function of temperature is illustrated in Figure 7(c). It is clearly seen that below the onset of  $\alpha'$  transition, RHDPE, RHDPE/CF/MA-g-HDPE, and RHDPE/CF/MA-g-HDPE/FACS composites showed relatively the same  $\tan \delta$  values and the curves overlay. It is after this point that the matrix and the composites curves start deviating from each other. A decreased magnitude of  $\tan \delta$  is obtained for the CF and both CF/FACS-filled composites in comparison with RHDPE matrix indicating less energy dissipation with a stronger interface<sup>40,56</sup> that becomes more pronounced at temperatures above  $\alpha'$  transition. The damping ( $\tan \delta$ ) values of RHDPE, RHDPE/CF, and RHDPE/CF/FACS composites compatibilized with MA-g-HDPE at the  $\alpha'$  transition temperature were 0.18, 0.15, and 0.14, respectively. Thus from DMA analysis, in FACS-filled RHDPE/CF/MA-g-HDPE composite, a good bonding at the filler–matrix interface was observed.

## CONCLUSIONS

The mechanical, thermal, dynamic mechanical, and water absorption properties of the RHDPE/CF/FACS biocomposites have been investigated along with fracture surface analysis.

- RHDPE/CF/FACS biocomposites were prepared using melt compounding technique.
- Composites prepared at 30 wt % of CF with 1 wt % MA-g-HDPE showed optimum mechanical performance. Incorporation of 7.5 wt % FACS gave a significant increase in flexural modulus and hardness in comparison with the RHDPE matrix.
- DSC measurements revealed that the fiber/FACS-reinforced RHDPE system displayed less  $T_m$ , which reveals the presence of a genuine interface. The  $T_c$  of the biocomposites showed significantly no change when compared with RHDPE matrix suggesting homogenous crystallization. The decreased melting enthalpy and crystallinity degree suggested an interaction of the fiber/FACS in the RHDPE matrix.

- The TGA and DTA thermograms also revealed an optimum thermal stability of the fiber/polymer system in presence of FACS.
- The storage and loss modulus values increased with the incorporation of the FACS in the RHDPE/CF composite with a decrease in damping factor.
- Tensile fractured surface observations showed that the FACS particles are well encapsulated in the RHDPE/CF composite matrix.
- For RHDPE/CF/FACS biocomposites, a good balance of properties in terms of stiffness and strength can be achieved at an optimal concentration of fibers, FACS, and MA-g-HDPE. The developed material can be advantageous for application in automobile interiors, false ceilings, floorings, and furniture.

## ACKNOWLEDGMENTS

Dr. Sukanya Satapathy thanks Department of Science and Technology (DST) for financial grant under Women Scientists Scheme-A (WOS-A), Grant No. SR/WOS-A/CS-91/2012 (G). Authors greatly acknowledge Central Institute of Plastics Engineering and Technology, Hyderabad, India for providing the processing and Izod impact testing facility for the composite samples.

## REFERENCES

1. Mutha, N. H.; Patel, M.; Premnath, V. *Resour. Conservat. Recycl.* **2006**, *47*, 222.
2. Satapathy, S.; Chattopadhyay, S.; Chakrabarty, K. K.; Nag, A.; Tiwari, K. N.; Tikku, V. K.; Nando, G. B. *J. Appl. Polym. Sci.* **2006**, *101*, 715.
3. Mitra, B. C. *Defence Sci. J.* **2014**, *64*, 244.
4. Thanomslip, C.; Hogg, P. J. *Compos. Sci. Technol.* **2003**, *63*, 467.
5. Wambua, P.; Ivens, J.; Verpoest, I. *Compos. Sci. Technol.* **2003**, *63*, 1259.
6. Lei, Y.; Wu, Q.; Yao, F.; Xu, Y. *Compos. Part A: Appl. Sci. Manufact.* **2007**, *38*, 1664.
7. Cui, Y.; Lee, S.; Noruziaan, B.; Cheung, M.; Tao, J. *Compos. Part A: Appl. Sci. Manufact.* **2008**, *39A*, 655.
8. Yao, F.; Wu, Q.; Lei, Y.; Xu, Y. *Indus. Crops Prod.* **2008**, *28*, 63.
9. Favaro, S. L.; Ganzerli, T. A.; De Carvalho Neto, A. G. V.; Da silva, O. R. R. F.; Radovanovic, E. *EXPRESS Polym. Lett.* **2010**, *4*, 465.
10. Oza, S.; Wang, R.; Lu, N. *IJAST* **2011**, *1*, 31.
11. Samariha, A.; Hemmasi, A. H.; Ghasemi, I.; Bazayr, B. *MEJSR* **2011**, *8*, 971.
12. Aht-Ong, D.; Atong, D.; Pechven, C. *Mat. Sci. Forum.* **2011**, *695*, 469.
13. Satapathy, S.; Nag, A.; Jose, J.; Nando, G. B. *J. Reinforc. Plast. Compos.* **2008**, *27*, 967.
14. Satapathy, S.; Nag, A.; Nando, G. B. *Prog. Rubber Plast. Recycl. Technol.* **2008**, *24*, 199.
15. Njoku, R. E.; Li, I. O.; Agbiogwu, D. O.; Agu, C. V. *Nigerian J. Technol.* **2012**, *31*, 107.
16. Rao, C. H. C.; Madhusudan, S.; Rahgavendra, G.; Rao, E. V. *IJERA* **2012**, *2*, 371.
17. Ayrilmis, N.; Jarusombuti, S.; Fueangvivat, V.; Bauchongkol, P.; White, R. H. *Fibers Polym.* **2011**, *12*, 919.
18. Karthikeyan, A.; Balamurugan, K. *JSIR* **2012**, *71*, 627.
19. Hussain, S. A.; Pandurangadu, V.; Palanikumar, K. *IJEST* **2011**, *3*, 7942.
20. Nam, T. H.; Ogihara, S.; Tung, N. H.; Kobayashi, S. *Compos. Part B* **2011**, *42*, 1648.
21. Bettini, S. H. P.; Bicudo, A. B. L. C.; Augusto, I. S.; Antunes, L. A.; Morassi, P. L.; Condotta, R.; Bonse, B. C. *J. Appl. Polym. Sci.* **2010**, *118*, 2841.
22. Fernandes, E. M.; Correlo, V. M.; Mano, J. F.; Reis, R. L. *Compos. Sci. Technol.* **2013**, *78*, 56.
23. Bhagat, V. K.; Biswas, S.; Dehury, J. *Polym. Compos.* **2014**, *35*, 925.
24. Zainudin, E. S.; Yan, L. H.; Haniffah, W. H.; Jawaid, M.; Alothman, O. Y. *Polym. Compos.* **2014**, *35*, 1418.
25. Deepthi, M. V.; Madan, S.; Sailaja, R. R. N. *Mater. Des., Des. Nanomat. Nanostruct.* **2010**, *31*, 2051.
26. Chand, N.; Sharma, P.; Mahi, F. *Mater. Sci. Eng. A* **2010**, *527*, 5873.
27. Satapathy, S.; Nag, A.; Nando, G. B. *Process Safety Environ. Protect.* **2010**, *88*, 131.
28. Satapathy, S.; Nag, A.; Nando, G. B. *Polym. Compos.* **2012**, *33*, 109.
29. Satapathy, S.; Nag, A.; Nando, G. B. *J. Appl. Polym. Sci.* **2013**, *130*, 4558.
30. Kulkarni, S. M.; Kishore, J. *J. Appl. Polym. Sci.* **2003**, *87*, 836.
31. Saxena, M.; Morchhale, R. K.; Asokan, P.; Prasad, B. K. J. *Compos. Mater.* **2008**, *42*, 367.
32. Subham, P.; Tiwari, S. K. *IJSER* **2013**, *4*, 1173.
33. Malkapuram, R.; Kumar, V.; Negi, Y. S. *J. Reinforc. Plast. Compos.* **2009**, *28*, 1169.
34. Nourbaksh, A.; Ashori, A. *J. Compos. Mater.* **2009**, *43*, 877.
35. Rozman, H. D.; Tay, G. S.; Kumar, R. N.; Abubakar, A.; Ismail, H.; Mohd. Ishak, Z. A. *Polym. Plast. Technol. Eng.* **1999**, *38*, 997.
36. Agunsoye, J. O.; Aigbodion, V. S. *Res. Physics* **2013**, *3*, 187.
37. Rana, A. K.; Mandal, A.; Bandyopadhyay, B. *Compos. Sci. Technol.* **2003**, *31*, 143.
38. Arsad, A.; Suradi, N. L.; Rahmat, A. R.; Danlami, J. M. *Int. J. Plas. Technol.* **2013**, *17*, 149.
39. Ishidi, E. Y.; Kolawale, E. G.; Sunmonu, K. O.; Yakubu, M. K.; Adamu, I. K.; Obele, C. M. *JETEAS* **2011**, *2*, 1073.
40. Biswal, M.; Mohanty, S.; Nayak, S. K. *J. Appl. Polym. Sci.* **2009**, *114*, 4091.
41. Santos, E. F.; Mauler, R. S.; Nachtigall, S. M. B. *J. Reinforc. Plast. Compos.* **2009**, *28*, 2119.
42. Brahmakumar, M.; Pavithran, C.; Pillai, R. M. *Compos. Sci. Technol.* **2005**, *65*, 563.

43. Tan, C.; Ahmad, I.; Heng, M. *Mater. Des.* **2011**, *32*, 4493.
44. Sengupta, S.; Maity, P.; Ray, D.; Mukhopadhyay, A. *J. Appl. Polym. Sci.* **2013**, *130*, 1996.
45. Pardo, S. G.; Bernal, C.; Area, A.; Abad, M. J.; Cano, J. *Polym. Compos.* **2010**, *31*, 1722.
46. Sreekanth, M. S.; Bambole, V. A.; Mhaske, S. T.; Mahanwar, P. A. *JMMCE* **2009**, *8*, 237.
47. Ray, D.; Bhattacharya, D.; Mohanty, A. K.; Drzal, L. T.; Misra, M. *Macromol. Mater. Eng.* **2006**, *291*, 784.
48. Nourbaksh, A.; Ashori, A. *J. Appl. Polym. Sci.* **2009**, *112*, 1386.
49. Patel, R. V.; Manocha, S. *J. Compos.* **2013**, *2013*, 1.
50. Mendes, L. C.; Cestari, S. P. *Mater. Sci. Appl.* **2011**, *2*, 1331.
51. Mattos, B. D.; Misso, A. L.; De Cademartori, P. H. G.; De Lima, E. A.; Magalhaes, W. L. E.; Gatto, D. A. *Construc. Building Mater.* **2014**, *61*, 60.
52. Tomczak, F.; sydenstricker, T. H. D.; Satyanarayana, K. G. *Compos. Part A* **2007**, *38*, 1710.
53. Mohanty, S.; Verma, S. K.; Nayak, S. K. *Compos. Sci. Technol.* **2006**, *66*, 538.
54. Ghasemi, I.; Kord, B. *Iranian Polym. J.* **2009**, *18*, 683.
55. Satapathy, S.; Nag, A.; Nando, G. B. *Int. J. Plast. Technol.* **2009**, *13*, 95.
56. Subham, P.; Tiwari, S. K. Proceedings of the International Conference on Advances in Aeronautical and Mechanical Engineering-AME **2012**, DOI:10.3850/978-981-07-2683-6AME-105, pp. 20-24.
57. Khanna, Y. P.; Turi, E. A.; Taylor, T. J.; Vickroy, V. V.; Abbott, R. F. *Macromolecules* **1985**, *18*, 1302.
58. Stehling, F. C.; Mandelkern, L. *Macromolecules* **1970**, *3*, 242.
59. Murayama, T. *Dynamic Mechanical Analysis of Polymeric Material*; Elsevier: Amsterdam, **1978**.
60. Behzad, M.; Tajvidi, M.; Ebrahimi, G.; Falk, R. H. *IJE Trans. B Appl.* **2004**, *17*, 95.